Spin States of Holes in Ge/Si Nanowire Quantum Dots

S. Roddaro, A. Fuhrer,* P. Brusheim, C. Fasth, H. Q. Xu, and L. Samuelson
Solid State Physics/The Nanometer Structure Consortium, Lund University, P.O. Box 118, S-221 00 Lund, Sweden

J. Xiang and C. M. Lieber
Department of Chemistry and Chemical Biology, Harvard University, Cambridge Massachusetts 02138, USA
(Received 29 May 2008; published 27 October 2008)

We investigate tunable hole quantum dots defined by surface gating Ge/Si core-shell nanowire heterostructures. In single level Coulomb-blockade transport measurements at low temperatures spin doublets are found, which become sequentially filled by holes. Magnetotransport measurements allow us to extract a g factor $g^* \approx 2$ close to the value of a free spin-1/2 particle in the case of the smallest dot. In less confined quantum dots smaller g factor values are observed. This indicates a lifting of the expected strong spin-orbit interaction effects in the valence band for holes confined in small enough quantum dots. By comparing the excitation spectrum with the addition spectrum we tentatively identify a hole exchange interaction strength $\chi \approx 130$ μeV.

DOI: 10.1103/PhysRevLett.101.186802 PACS numbers: 73.23.Hk, 73.63.Kv, 73.63.Nm

Nanoparticle-mediated growth of nanowires (NWs) has been at the center of a significant experimental effort in the past years [1,2] and is leading to the development of new classes of devices [1–8] that are receiving growing attention both as research tools and for their potential applications. Coaxial Ge/Si NWs constitute a special case as they support a high-mobility one-dimensional hole gas with a mean free path exceeding 170 nm even at room temperature [1,3,6]. Holes are also expected to have interesting transport characteristics in regard to their spin degrees of freedom: the spin-orbit (SO) interaction is much stronger in the valence band and spin and orbital motion are usually intrinsically linked [9–12]. However, through the Broido-Sham transformation, the 4×4 Luttinger Hamiltonian can be brought to block form, defining a pseudospin (generalized parity) quantum number analogous to the electron 1/2 spin [13]. Such pseudospin states are typically characterized by a complex spatial spin texture and their coupling to the magnetic field is predicted to be anisotropic as well as strongly state dependent [14]. Here, we report on tunable gated Ge/Si-nanowire quantum dots (QDs) in which we find sequential filling of spin doublets with a g factor close to the value of a free spin-1/2 particle in the case of a small enough dot. This indicates a lifting of the expected strong spin-orbit interaction effects in the valence band for strongly confined holes and by comparing the excitation spectrum with the addition spectrum of the quantum dot we tentatively identify an exchange interaction strength $\chi \approx 130$ μeV for the holes. Together with their superior transport properties and local gate control this makes Ge/Si nanowires ideal systems for coherent manipulation and coupling of spins by control of the spin-orbit and exchange interaction. Note that in the following we use the term *spin* in a more general way without explicitly differentiating to pseudospin in the sense of a generalized parity symmetry.

Our Ge/Si NWs were grown in a two-step chemical vapor deposition process: in the first step Ge NWs with a diameter of 15 ± 4 nm were fabricated by gold nanocluster assisted growth; in the second step the NW surface was passivated by overgrowing a Si shell with a thickness of 1.5 to 2 nm. The valence band offset between Ge and Si ($\Delta E_V \approx 500$ meV) leads to a natural population of holes in the Ge core such that intentional doping can be avoided, which results in greatly improved transport properties. Further details on the growth and NW structure have been reported previously [1]. NWs were dispersed in ethanol from the growth substrate by sonication and deposited on a degenerately doped Si substrate with a 600 nm-thick thermal oxide layer. They were then located in relation to predefined markers using a scanning electron microscope and contacted by electron beam lithography, with annealed Ni Ohmic contacts [1]. A HfO_2 dielectric layer with a thickness of 25 ± 5 nm was deposited over the NWs and contacts, and then seven 50 nm-thick Ti/Au gate fingers were placed on top of the encapsulated structure as shown in Fig. 1(a).

Five gate electrodes $g_1 - g_5$ [blue in Fig. 1(a)] were used to locally tune the band edge positions to form tunable tunnel barriers and adjust the hole density within the wire. These gates were 50 nm wide with a periodicity of 80 nm and were aligned to lie within the 800 nm-wide gap between the Ohmic contacts [yellow in Fig. 1(a)]. Two larger gates g_S and g_D (red), partially overlapping the Ohmic contacts, were kept at negative voltages close to -5.0 V in order to maintain a high hole density and thus ensure good carrier injection into the NW even for large positive voltages on the inner gate electrodes. Low temperature transport measurements were performed in a dilution refrigerator with base temperatures of 80 mK.

By tuning the five gate voltages $V_{g1} - V_{g5}$ a variety of single and double dot configurations can be obtained along

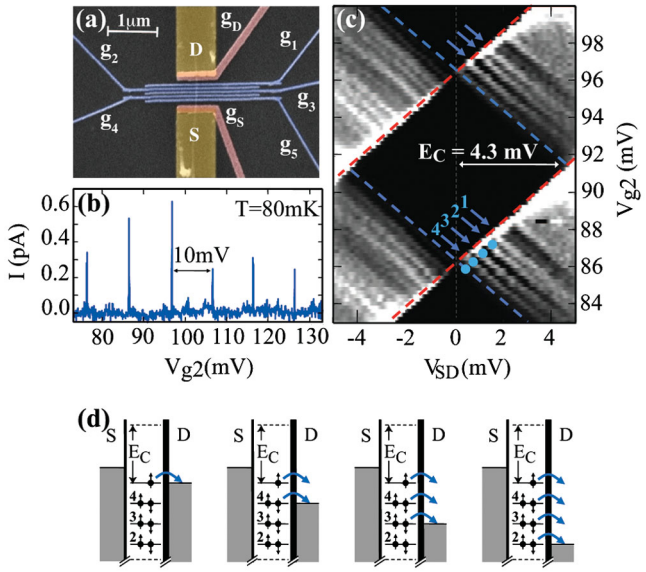

FIG. 1 (color). (a) Scanning electron microscope image in artificial colors of one of the devices. (b) Coulomb blockade oscillations for a quantum dot confined between barrier electrodes g_1 ($V_{g1} = +2.40$ V) and g_3 ($V_{g3} = +2.60$ V) measured with a source-drain bias $V_{SD} = 100$ μV. The inter peak spacing is $\Delta V_{g2} \approx 10$ mV with small fluctuations due to quantum confinement. (c) Coulomb blockade diamonds in the same regime as in (b). Excited state lines with $\Delta\epsilon \approx 380 \pm 60$ μeV are clearly visible on the right side of the diamonds with an average charging energy $E_C = 4.3 \pm 0.1$ meV. (d) Single-particle picture of the hole tunneling process leading to the excited states in panel (c).

the NW [15,16]. In this Letter we focus on the simplest situation of a single quantum dot induced by biasing gates $g1$ and $g3$ close to pinch-off (+2.40 and +2.60 V, respectively) and using gate $g2$ as a plunger gate in the range 50–150 mV. Figure 1(b) shows a measurement of the current through the NW as a function of plunger gate voltage V_{g2}, exhibiting pronounced Coulomb blockade oscillations with an average separation of $\Delta V_{g2} \approx 10$ mV. From the typical pinch-off voltages of the gates on this device ($\approx$2.0 V) and the average peak separation ΔV_{g2} we estimate that the quantum dot for plunger gate voltages $V_{g2} \approx 0$ mV contains about 100 holes. Figure 1(c) shows the corresponding Coulomb diamonds in the differential conductance through the NW as a function of V_{g2} and a symmetrically applied dc bias V_{SD} with $V_S = +V_{SD}/2$ and $V_D = -V_{SD}/2$. From the extent of the diamonds we determine an average charging energy $E_C = e/C_\Sigma \approx 4.3$ meV, which corresponds to a total dot capacitance $C_\Sigma \approx 37$ aF. The plunger gate lever arm $\alpha_{g2} = C_{g2}/C_\Sigma \approx 0.445$ was obtained from the difference between the two borderline slopes crossing where the diamonds touch at $V_{SD} = 0$ [see blue and red dashed lines in Fig. 1(c)]. The plunger gate capacitance can be evaluated as $C_{g2} = e/\Delta V_{g2} \approx 16$ aF and in a similar way the barrier gates give $C_{g1} = 12$ aF and $C_{g3} = 7$ aF. This leaves only a negligibly small capacitive coupling $C_\Sigma - C_{g1} - C_{g2} - C_{g3} \approx 1$ aF for the S and D leads of the device and the buried degenerately doped Si substrate.

Clear excitation lines are visible in Fig. 1(c) running parallel to the blue dashed line at large bias voltages $|V_{SD}|$. These excitation lines are related to tunnel processes between the dot and the drain contact. Similar excitation lines could be expected to run parallel to the red dashed line (alignment of dot levels with source), but we adjust the gate voltages such that the tunnel coupling between the dot and the source contact is much stronger and excitations parallel to the red borderline are not visible. This makes it considerably easier to interpret the excitation spectrum. The excitation lines on the right-hand side of the diamonds, on which we will put the main focus, are due to *emission* (dot $\rightarrow$ lead) processes from an increasing number of dot levels as the V_{SD} is increased. In contrast to this, excitations in the left part of the diamonds can be interpreted in terms of *absorption* (lead $\rightarrow$ dot) of holes into the dot's excited states. Figure 1(d) shows the level alignment in a simple single-particle picture for the four blue dots in Fig. 1(c), starting from the lowest dot which indicates the ground-state. In this picture every resonance in the differential conductance corresponds to a new quantum level that becomes available for transport through the dot-drain barrier.

In Fig. 2(a) we look more closely at an extended sequence of Coulomb blockade diamonds for the same dot configuration in order to investigate the spin filling in this dot. We argue that the evolution of the emission excitation lines suggests an interpretation in terms of sequential filling of spin degenerate hole states in the dot. We start our analysis by observing that the *emission* spectrum on the right side of the diamonds contains a slightly wider stripe of low differential conductance (black) which we mark with a blue triangle. As the dot is depleted of holes (towards more positive V_{g2}) the wider stripe moves towards the ground state (blue dashed line) consistent with a depopulation of quantum levels. For a more quantitative discussion we take diagonal cuts through the emission spectrum averaging along the excitation lines over the green shaded area. Figure 2(b) shows these cuts for each diamond in the left panel. Since the diamonds are near perfectly symmetric we use $E = eV_{SD} - E_0$ to define the energy axis, where E_0 is the ground-state energy after averaging [indicated by the blue arrow in Fig. 2(b)] and V_{SD} is taken for each point along the diagonal cut. As before, the emission spectra in Fig. 2(b) show clearly that the wide minimum marked by the blue triangle moves towards $E = 0$ as the dot gets depleted. We define the excitation line to the left of this minimum to be from level N_0 and count the excited states at higher energy from this point upwards (towards the left from level N_0). Comparing the different cuts shows clearly that lines disappear one by

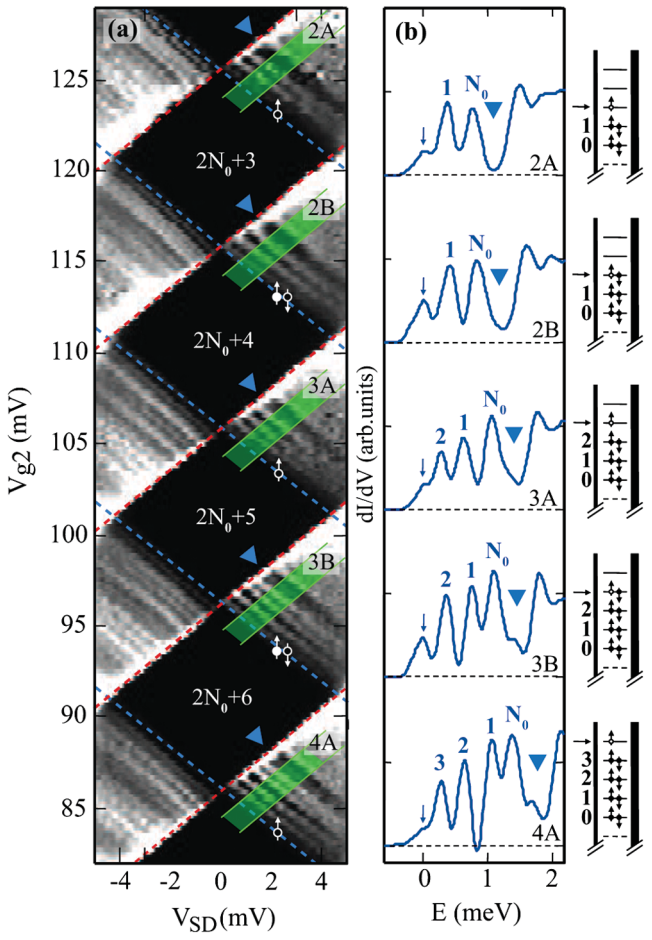

FIG. 2 (color). (a) Coulomb-blockade diamonds in the same gate configuration as in Fig. 1. (b) Cross sections of the emission spectrum averaged along the excitation lines over the green shaded area shown in Fig. 2(a). The corresponding hole configuration on the dot is indicated at the right of the figure.

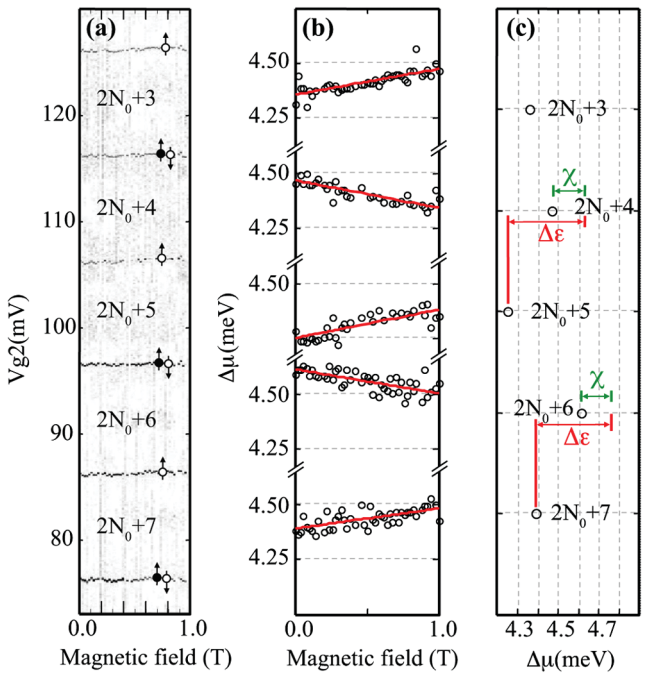

FIG. 3 (color). (a) Coulomb blockade peak evolution for different values of an external magnetic field applied perpendicular to the nanowire axis. (b) Evolution of the addition energy for different hole configurations on the QD. (c) Ground-state addition spectrum at $B = 0$ T. The black circles mark the addition energies extracted from (a). The red arrows indicate the single-particle energy $\Delta\epsilon$ as extracted from the excitation spectrum. The difference can be explained by an exchange interaction contribution χ.

one for every *two* holes that are removed from the dot. Following this observation, we mark similar spectra with the same number $2A$, $2B$, etc., using A and B to distinguish between the two occurrences of the same resonance curve (at lower and higher hole filling, respectively). This evolution can be interpreted as the sequential filling of spin doublets on level n where nA corresponds to the emission from a dot configuration with a singly filled topmost spin state and nB to one with a fully occupied topmost level. Such a picture also explains the regular oscillation of the amplitude of the first peak (arrow) on curves in Fig. 2(b). The peak is always higher for nB curves and smaller for nA curves, in agreement with the number of spin channels available for tunneling out through the drain tunnel-barrier in the two cases. Following this analysis we label the diamonds in Fig. 2(a) using even or odd hole numbers and indicate the expected spin filling on the right of Fig. 2(b).

To further support the sequential spin filling picture, Fig. 3(a) shows the evolution of the same Coulomb blockade peaks as in Fig. 2 as a function of a magnetic field B applied perpendicular to the nanowire. In agreement with our interpretation, $\Delta\mu(B) = e\alpha_{g2}\Delta V_{g2}(B)$ values corresponding to even and odd spin filling configurations in Fig. 3(b) evolve in opposite directions as a function of B. In a constant interaction approximation, the Coulomb gap is expected to be $\Delta\mu(B) = e^2/C_\Sigma + \Delta\epsilon(B)$, where $\Delta\epsilon(B)$ is the energy difference between quantum states involved in tunneling at $V_{SD} = 0$. For odd spin filling one expects $\Delta\epsilon(B) = |g_n^*\mu_B B|$ while for even spin filling $\Delta\epsilon(0) > 0$ and $\Delta\epsilon(B) = \Delta\epsilon(0) - |g_n^*\mu_B B|/2 - |g_{n+1}^*\mu_B B|/2$. Here n and $n+1$ refer to the index of the quantum level being filled on the Coulomb peak below and above the corresponding Coulomb diamond. Allowing for spin-orbit coupling effects we assume that the g factors for each orbital level can be different [14]. A fit of the data in Fig. 3(b) using three independent g factor values for the three spin degenerate levels yields $|g_{N_0+2}^*| = 2.0 \pm 0.4$, $|g_{N_0+3}^*| = 2.2 \pm 0.4$, and $|g_{N_0+4}^*| = 1.6 \pm 0.4$. Given the uncertainties, we conclude that the observed g factors are close to the value expected for a free spin $1/2$ particle. This is also similar to p-type quantum dots in silicon-nanowires [17] even though in contrast to silicon hole states in bulk Ge are

found to have strongly enhanced g factors due to the spin-orbit interaction [18].

In a constant interaction picture at $B = 0$ T the Coulomb gaps with an odd number of holes are expected to be smaller since they reflect only the Coulomb interaction between two particles on the same orbital. This is qualitatively consistent with the values $\Delta\mu(0)$ shown on panel (c) as circle marks (○) for $B = 0$ T. However, even these values vary slightly from state to state showing the limited validity of such a simple approximation. To move beyond the constant interaction approximation we note that the two pseudospin blocks of the Hamiltonian are spanned by orthogonal 3/2-angular-momentum spinors [14]. Since the Coulomb potential is diagonal in spinor space, the Hartree-Fock approximation readily generalizes to holes, with vanishing Coulomb overlap integral between opposite pseudospins, analogous to the electron spin. In this language both fluctuations in the direct Coulomb term and exchange contributions are expected for such a quantum dot [19,20]. If we extract the level spacing from the excited state lines in Fig. 2(b) we find consistent values of $\Delta\epsilon = 380\ \mu\text{eV} \pm 60\ \mu\text{eV}$, indicated by the red arrows in Fig. 3(c). This is about 130 μeV larger than the variation that we find between even and odd hole numbers from the analysis of the ground-state peaks. Specifically, for even Coulomb gaps the exchange contribution per particle χ enters as $\Delta\mu_{2n} = \Delta\epsilon_n + C - \chi$ while for odd Coulomb gaps it does not contribute and $\Delta\mu_{2n-1} = C$ only contains the Hartree contribution C. This makes the difference between even and odd Coulomb gap energies $\Delta\epsilon_n - \chi$ and thus allows us to tentatively extract $\chi \approx 130\ \mu$eV as indicated in Fig. 3(c) by the green arrows. We note that the splitting of the excited state lines in Fig. 2(b) will in general also be affected by exchange and fluctuations in Hartree. However, for even electron numbers [nB in Fig. 2(a)] the splitting does not contain—on average—a significant interaction contribution since fluctuations in the direct Coulomb terms are expected to be small for a many hole system and with a similar argument exchange does not influence the splitting as long as all quantum levels are doubly occupied with two spins of opposite sign [19].

In conclusion our results consistently indicate the presence of degenerate spin states in dots with strong confinement along the nanowire axis. These spin states are sequentially filled with spin-up and spin-down and exhibit a g factor close to the value expected for a free spin-1/2 particle. This contrasts values which we observe in other experiments with larger quantum dots where $|g^*|$ was found to be considerably suppressed [16]. However, in both cases we find linear splittings as a function of magnetic field up to $B = 8$ T. While our estimate of the exchange energy $\chi \approx 130\ \mu$eV has to remain tentative due to the limited number of data-points available, we expect that these results will stimulate further work towards the utilization of holes in spintronic devices, where spin-orbit strength and exchange interaction are decisive factors for the coherent manipulation of spin states.

The authors wish to acknowledge helpful discussions with U. Zülicke and D. Csontos (Massey University, New Zealand). This work was supported by the Swedish SSF and VR, the Office of Naval Research (ONR), the Swiss SNF, and Italian MIUR (Projects No. II04CBCF18 and No. RBIN045MNB).

*fuhrer@nigra.ch

[1] J. Xiang, W. Lu, Y. Hu, Y. Wu, H. Yan, and C. M. Lieber, Nature (London) **441**, 489 (2006).
[2] T. Bryllert, L.-E. Wernersson, T. Löwgren, and L. Samuelson, Nanotechnology **17**, S227 (2006).
[3] W. Lu, J. Xiang, B. P. Timko, Y. Wu, and C. M. Lieber, Proc. Natl. Acad. Sci. U.S.A. **102**, 10 046 (2005).
[4] A. Fuhrer, L. E. Fröberg, J. N. Pedersen, M. W. Larsson, A. Wacker, M.-E. Pistol, and L. Samuelson, Nano Lett. **7**, 243 (2007).
[5] C. Fasth, A. Fuhrer, M. T. Björk, and L. Samuelson, Nano Lett. **5**, 1487 (2005).
[6] J. Xiang, A. Vidan, M. Tinkham, R. M. Westervelt, and C. M. Lieber, Nature Nanotech. **1**, 208 (2006).
[7] A. Pfund, I. Shorubalko, R. Leturcq, and K. Ensslin, Appl. Phys. Lett. **89**, 252106 (2006).
[8] M. T. Björk, A. Fuhrer, A. E. Hansen, M. W. Larsson, L. E. Fröberg, and L. Samuelson, Phys. Rev. B **72**, 201307(R) (2005).
[9] R. Winkler, *Spin-Orbit Coupling Effects in 2D Electron and Hole Systems* (Springer, Berlin, 2003).
[10] R. Danneau, O. Klochan, W. R. Clarke, L. H. Ho, A. P. Micolich, M. Y. Simmons, A. R. Hamilton, M. Pepper, D. A. Ritchie, and U. Zülicke, Phys. Rev. Lett. **97**, 026403 (2006).
[11] C. E. Pryor and M. E. Flatté, Phys. Rev. Lett. **96**, 026804 (2006).
[12] K.-M. Haendel, R. Winkler, U. Denker, O. G. Schmidt, and R. J. Haug, Phys. Rev. Lett. **96**, 086403 (2006).
[13] D. A. Broido and L. J. Sham, Phys. Rev. B **31**, 888 (1985).
[14] D. Csontos and U. Zülicke, Phys. Rev. B **76**, 073313 (2007).
[15] Y. Hu, H. O. H. Churchill, D. J. Reilly, J. Xiang, C. M. Lieber, and C. M. Marcus, Nature Nanotech. **2**, 622 (2007).
[16] See EPAPS Document No. E-PRLTAO-101-042844 for supplementary information on less confined Si/Ge NW quantum dots and tunable double quantum dots. For more information on EPAPS, see http://www.aip.org/pubservs/epaps.html.
[17] Z. Zhong, Y. Fang, W. Lu, and C. M. Lieber, Nano Lett. **5**, 1143 (2005).
[18] J. C. Hensel, Phys. Rev. Lett. **21**, 983 (1968).
[19] A. Fuhrer, T. Ihn, K. Ensslin, W. Wegscheider, and M. Bichler, Phys. Rev. Lett. **91**, 206802 (2003).
[20] S. Tarucha, D. G. Austing, Y. Tokura, W. G. van der Wiel, and L. P. Kouwenhoven, Phys. Rev. Lett. **84**, 2485 (2000).